

Supplementary Material

Self-powered p-CuBr/n-Si Heterojunction Photodetector Based on Vacuum Thermally Evaporated High-quality CuBr Films

Bin Xia^a, Lichun Zhang^{a,b*}, Dan Tian^a, Shunli He^a, Ning Cao^a, Guanying Xie^b, Dengying Zhang^a,
Xinbo Chu^{b*}, Fengzhou Zhao^{a*}

^a School of Physics and Optoelectronic Engineering, Ludong University, Yantai, 264025, China

^b School of integrated circuits, Ludong University, Yantai, 264025, China

* Corresponding author.

Email-address: phyzlc@163.com

Email-address: chuxinbo007@163.com

Email-address: fzzhao@ustc.edu

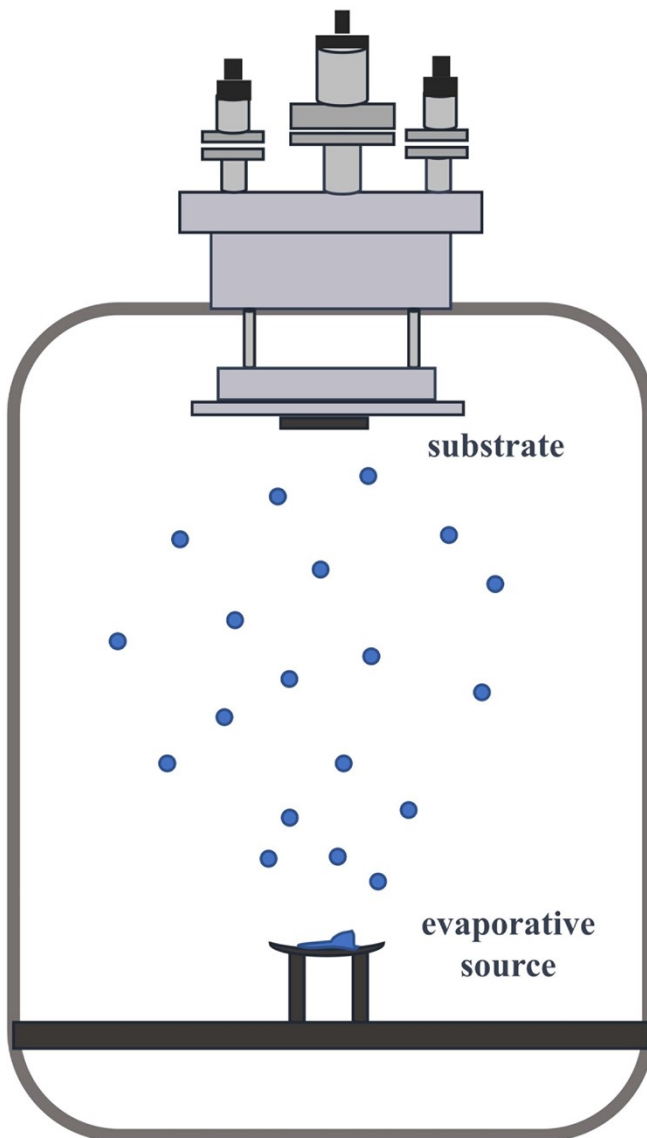


Fig. S1 Schematic Diagram of Vacuum Thermal Evaporation.

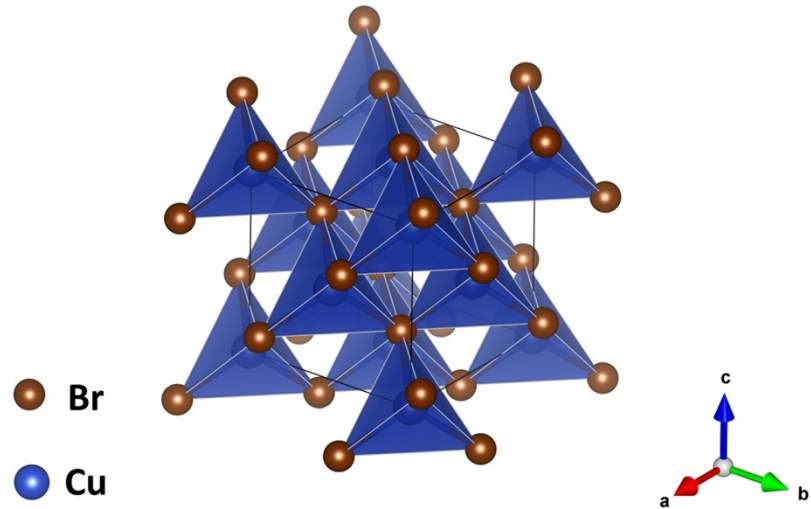


Fig. S2 Schematic diagram of CuBr crystal structure.

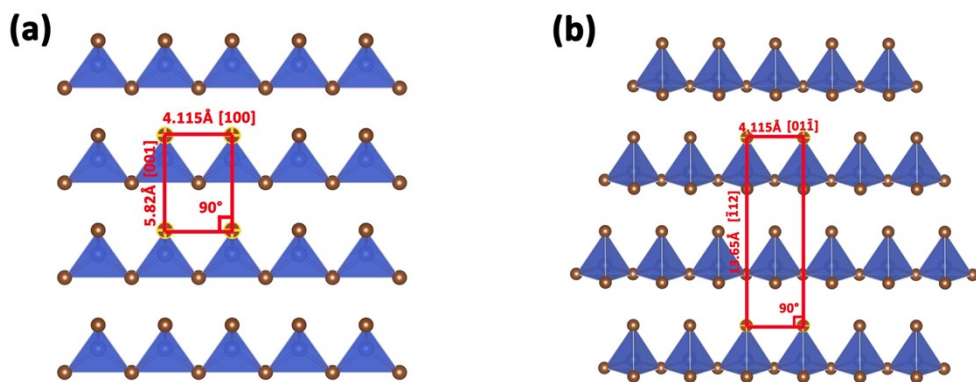


Fig. S3 (a)CuBr (220) crystal plane, (b) CuBr(311) crystal plane.

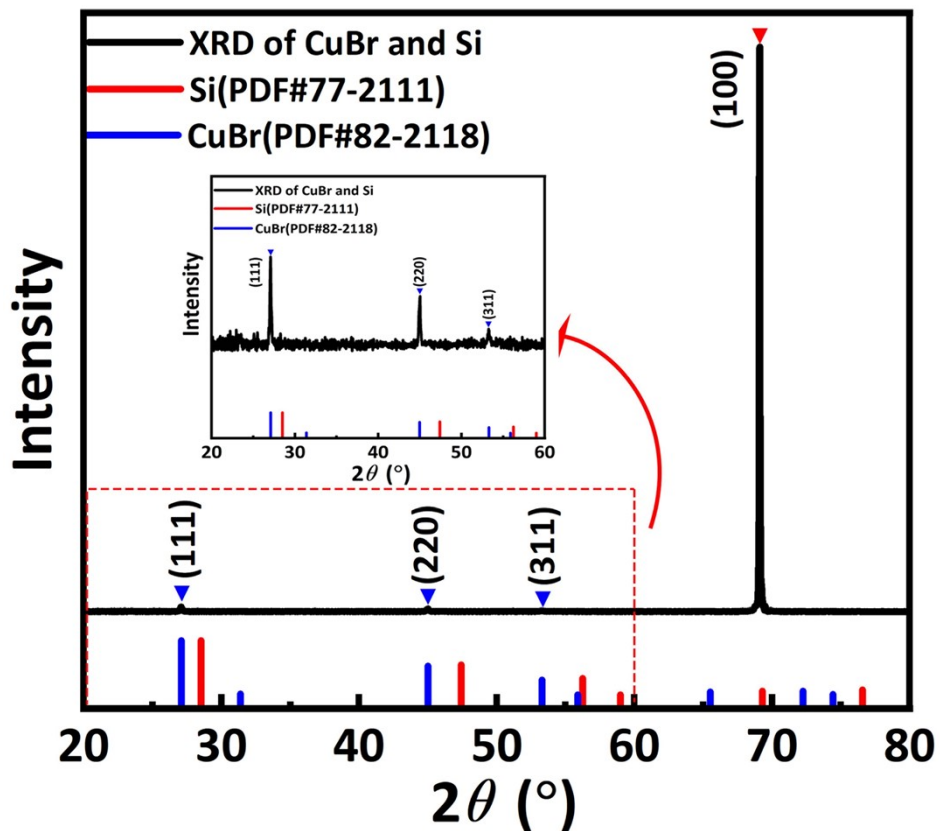


Fig. S4 XRD patterns of CuBr films with unshielded Si signals.

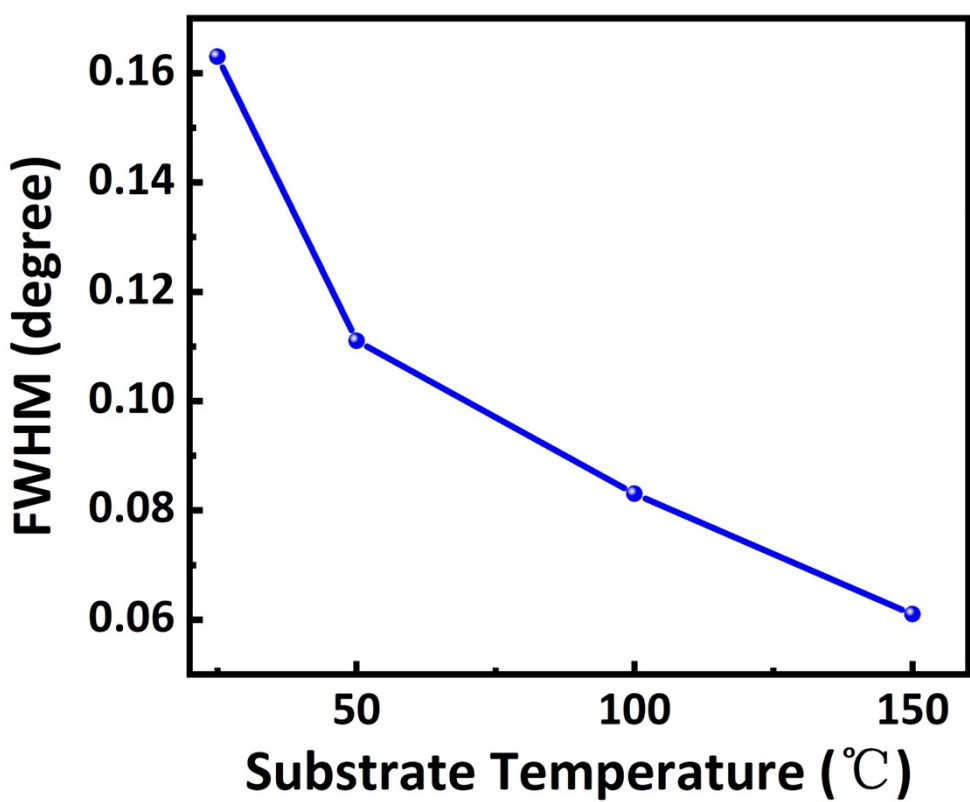


Fig. S5 the FWHM of (111) diffraction peaks at different substrate temperatures.

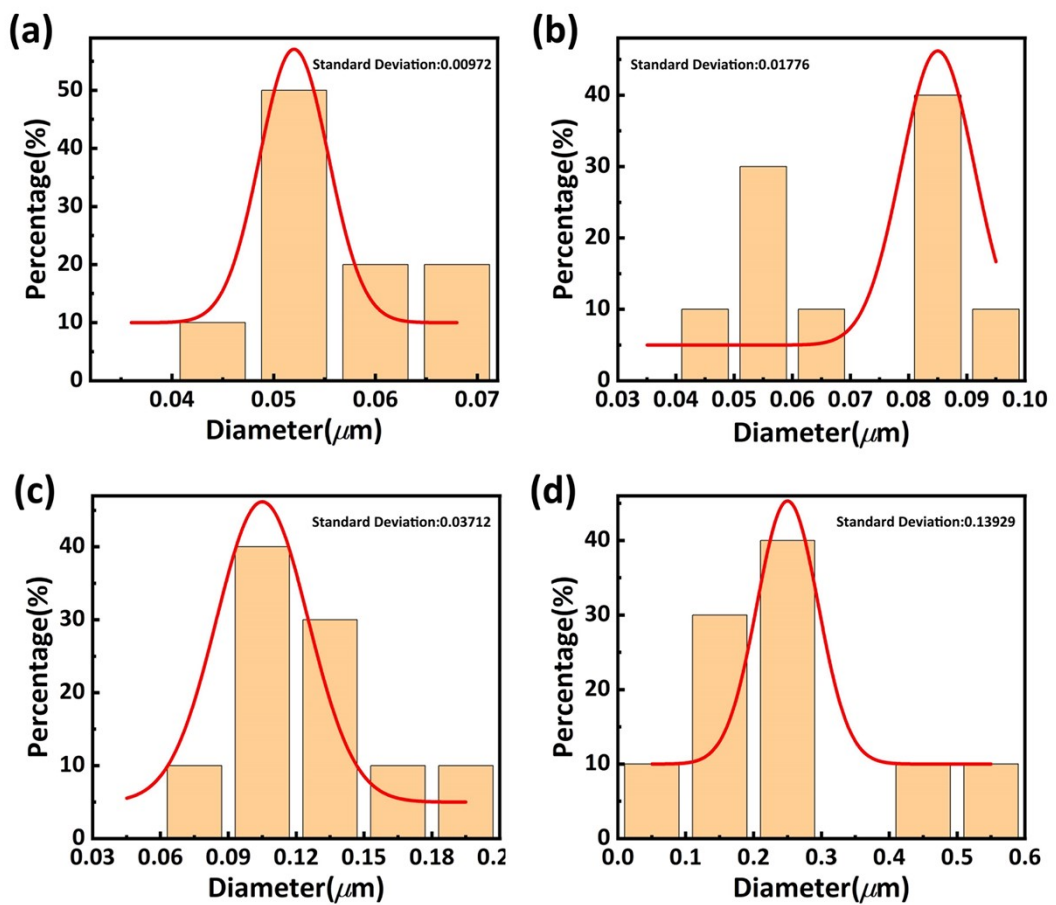


Fig. S6 Histogram of grain size at different substrate temperatures. (a)RT,(b) 50°C,(c)100°C,(d)150°C.

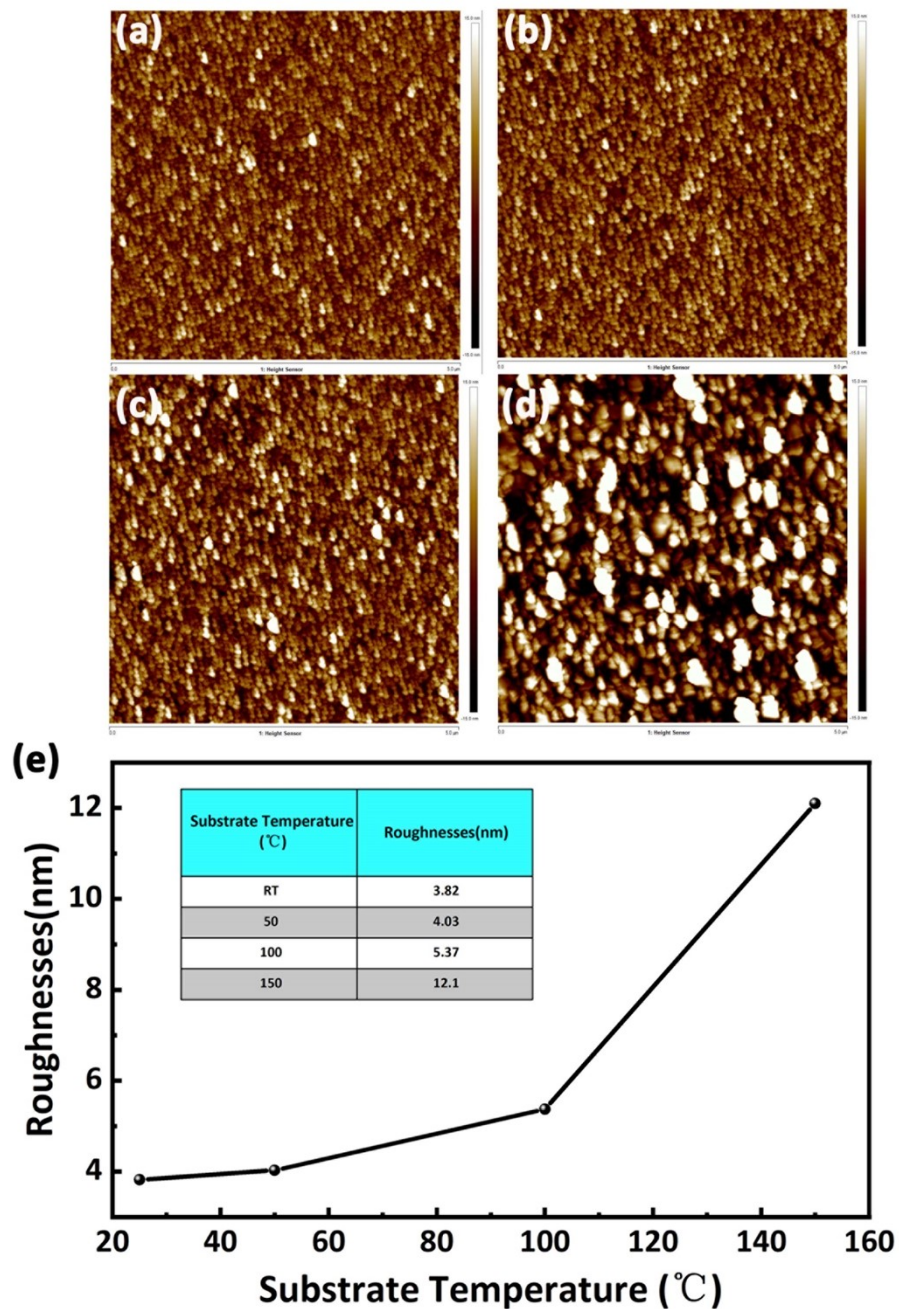


Fig. S7 AFM images of CuBr films. (a)RT,(b) 50°C,(c)100°C,(d)150°C,(e) Roughness at different substrate temperatures.

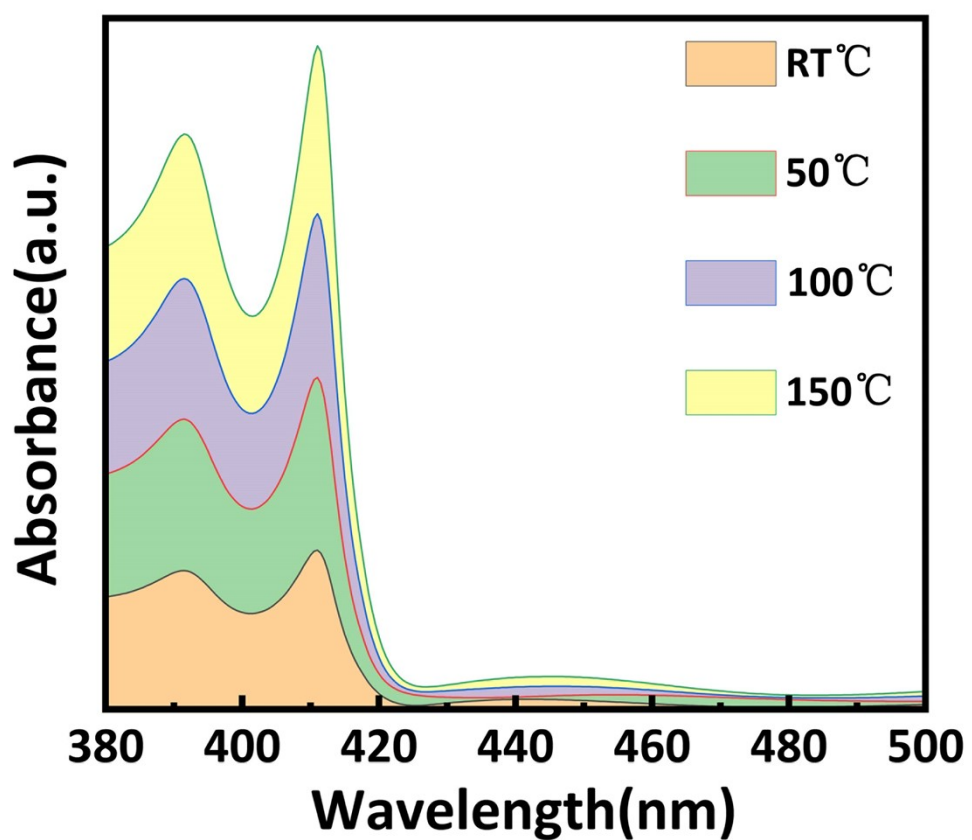


Fig. S8 Absorption spectra of CuBr thin films grown at different substrate temperatures.

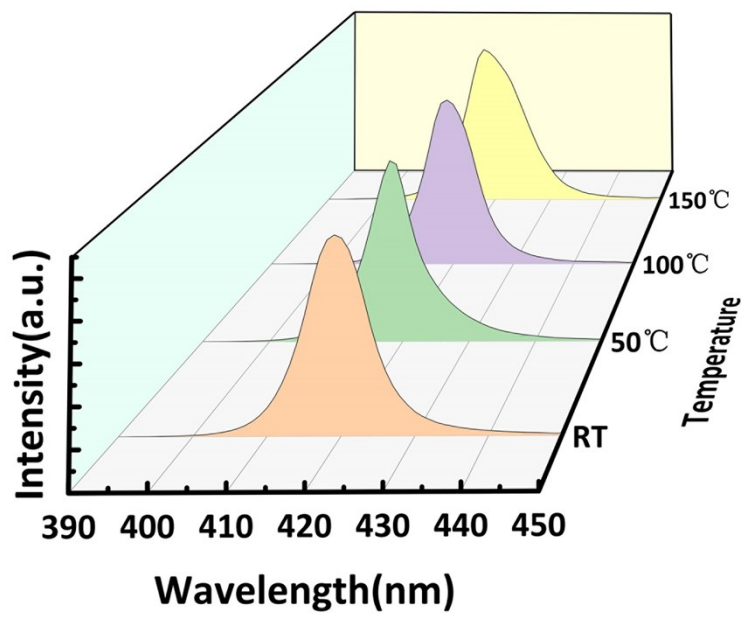


Fig. S9 Photoluminescence spectra of CuBr film grown at different substrate temperatures.

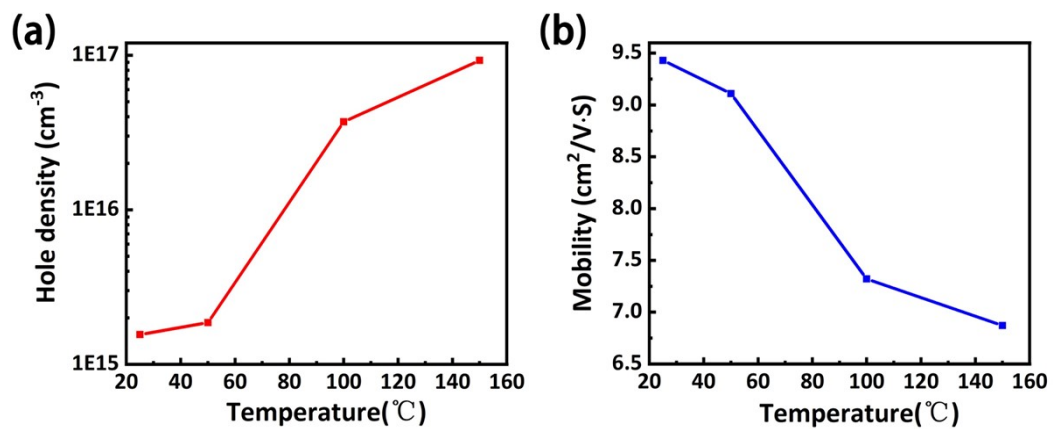


Fig. S10 CuBr at different substrate temperatures (a) hole concentration,(b) mobility.

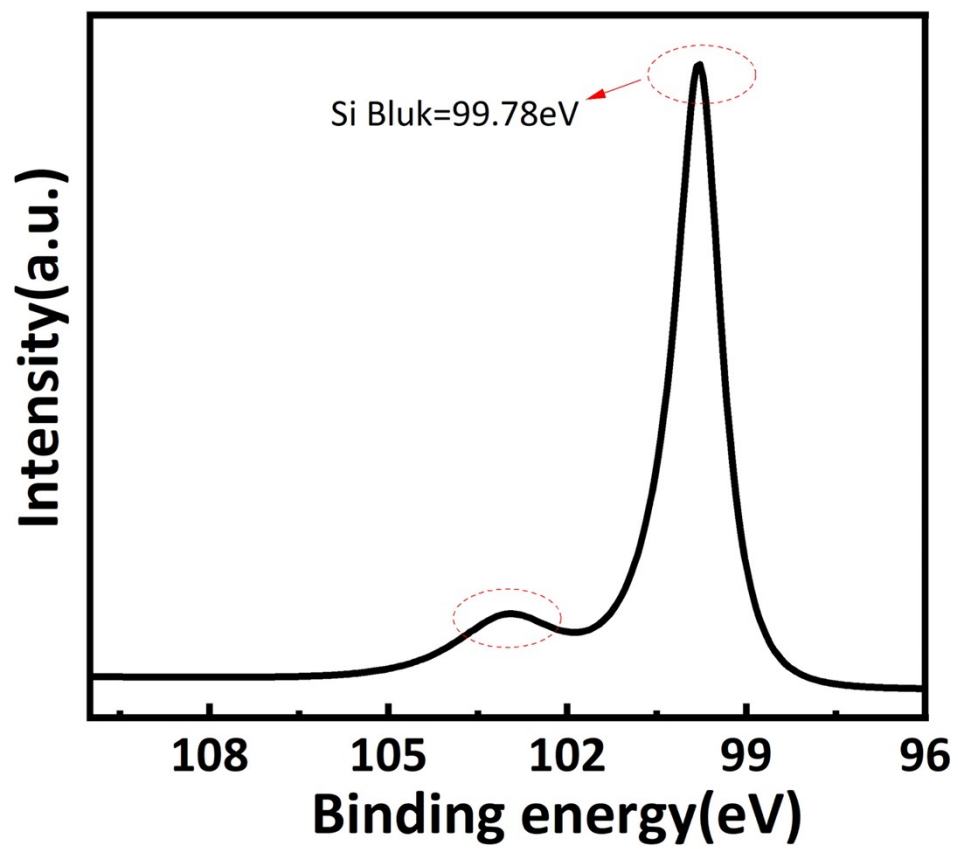


Fig. S11 Si 2p spectrum measured by XPS

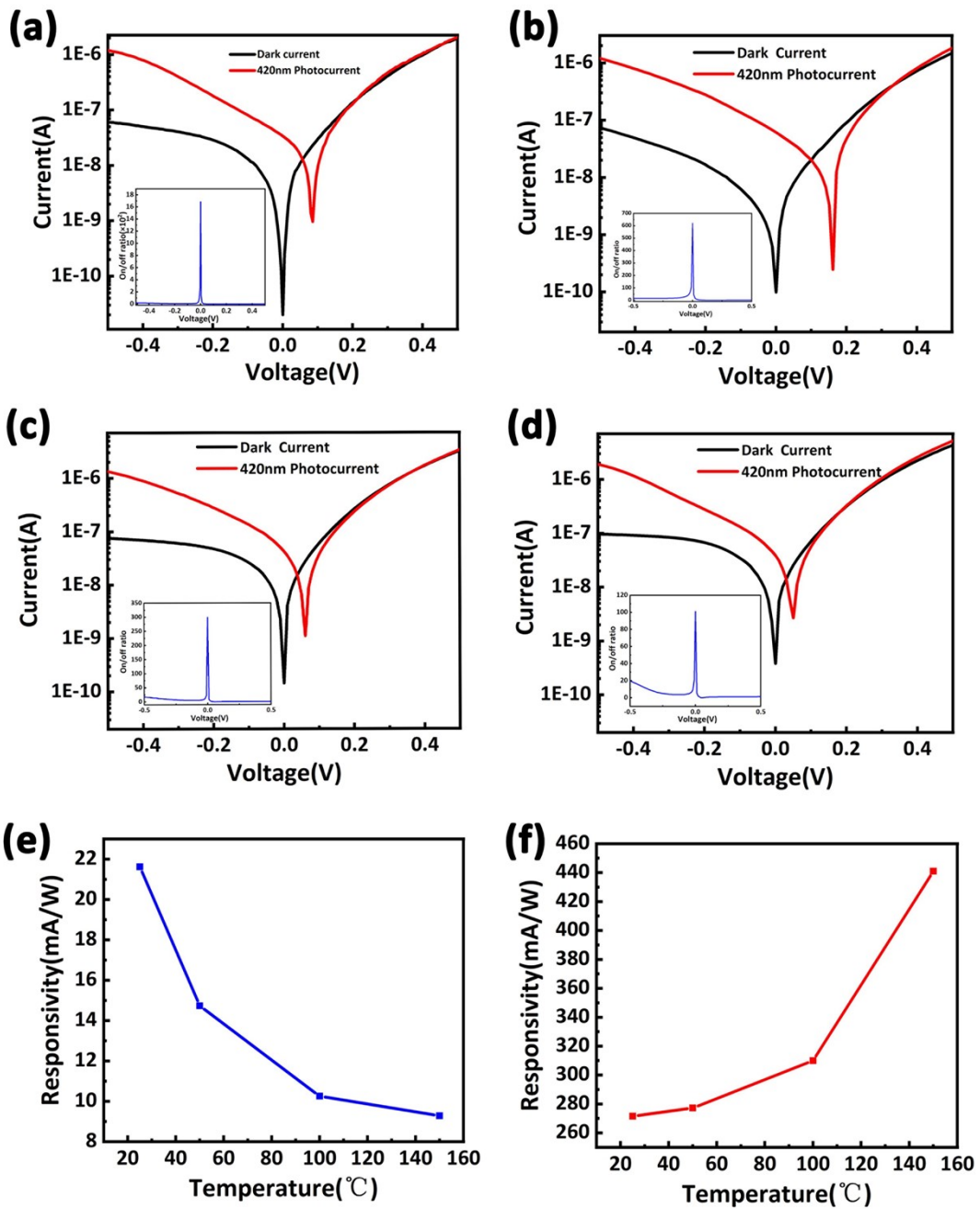


Fig. S12 (a) light-dark current and switching ratio at RT, (b) light-dark current and switching ratio at 50 °C, (c) light-dark current and switching ratio at 100 °C, (d) light-dark current and switching ratio at 150 °C; (e) responsivity versus substrate temperature at 0V, and (f) responsivity versus substrate temperature at -0.5V

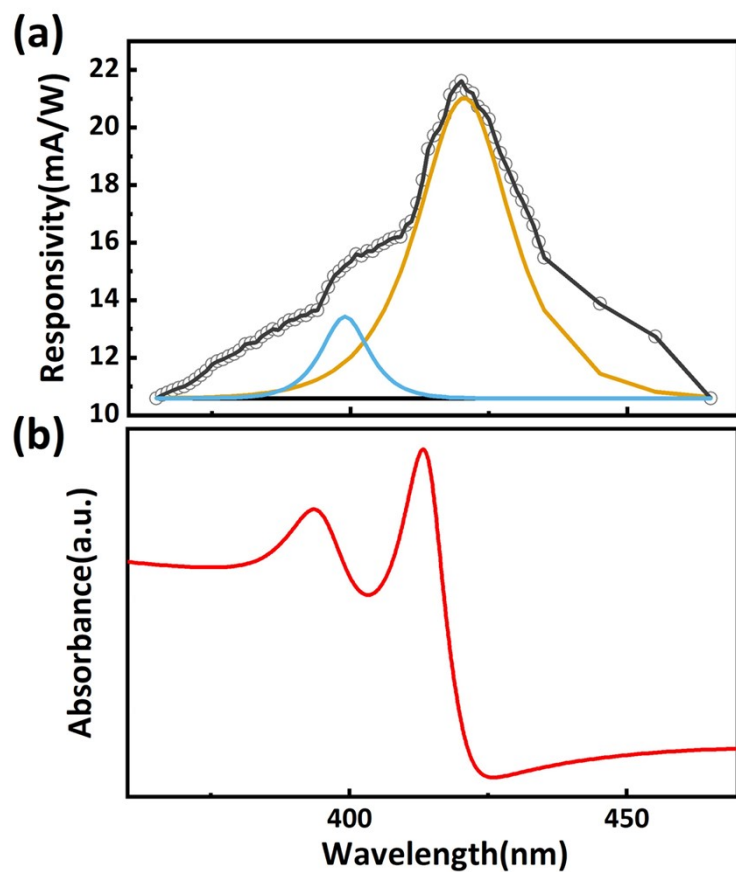


Fig. S13 (a) Spectral responsivity of CuBr/n-Si device at zero bias voltage,(b) UV-Visible absorption spectrum of CuBr thin film deposited under RT

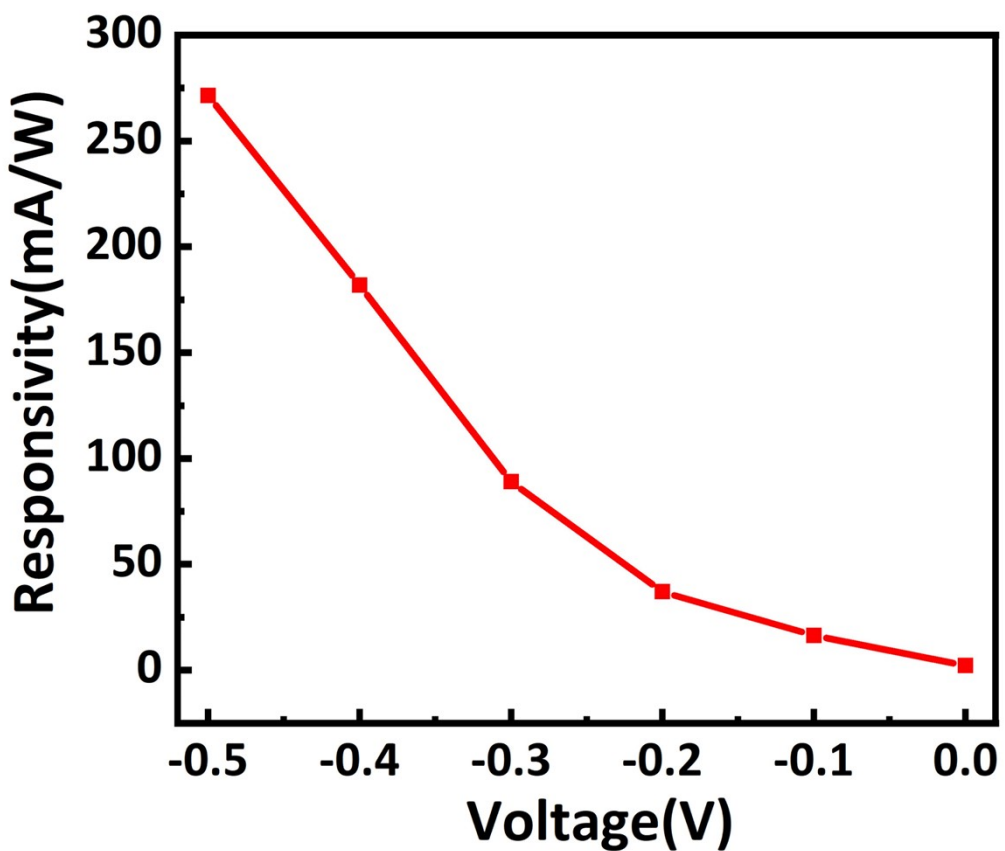


Fig. S14 Device responsiveness at different bias voltages

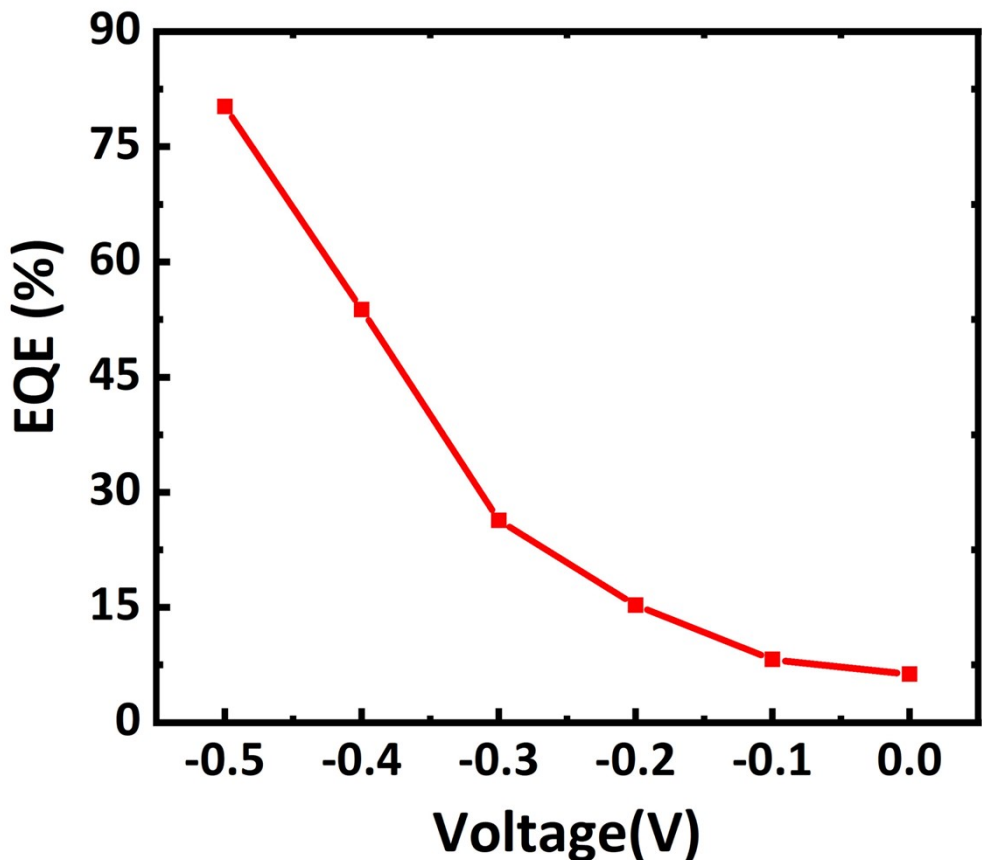


Fig. S15 EQE under different biases.

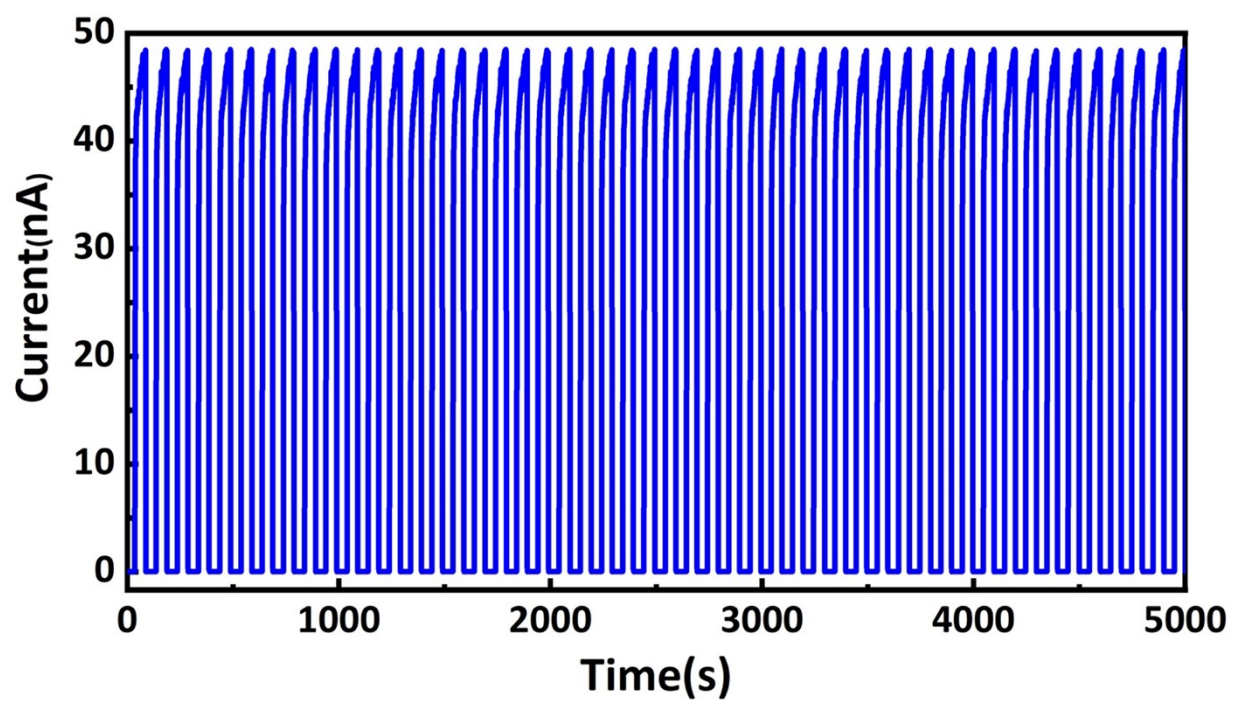


Fig. S16 The current-time curve of the device over 50 cycles at 0V bias.

Table. S1 Comparison of key parameters of CuBr or CuI based photodetectors

Device structure	Wavelength h (nm)	R(A/W)	D* ($\times 10^{12}$ Jones)	Bias(V)	EQE	On/off ratio	Rise/decay time(ms)	Ref.
CuBr/Ag	345	3.17	0.14	0	1126%	—	48/32	1
CuI/ZnO	385	0.235	1.23	-5	—	5500	80/84	2
CuI/Si	365	0.00126	—	0	—	80.8@-3V	—	3
CuI/GaN	360	0.0755	1.27	0	—	2320	160/158	4
ZnONRs/CuI	380	0.08684	—	0	-2V/ 14388%	—	110/110	5
CuI/a-IGZO	365	0.0002~ 0.0003	—	0	—	130~350	—	6
TiO ₂ /Si	365	26	1.31	-4	—	—	0.1276/0.12 03	7
CuBr/Si	420	0.0216	0.53	0	6.3%	1689	18.6/12.8	This work

References

1. C. Gong, J. Chu, C. Yin, C. Yan, X. Hu, S. Qian, Y. Hu, K. Hu, J. Huang and H. Wang, *Adv. Mater.*, 2019, 31, 1903580.
2. S. Niu, F. Zhao, Y. Hang, C. Wang, L. Xin, M. Zhang, M. Xu, D. Zhang, X. Chu and L. Zhang, *Optics Letters*, 2020, 45, 559-562.
3. Z. Li, L. Zhang, J. Wang, L. Yang, L. Xin, G. Li, G. Lin, S. Niu, J. Yan and F. Zhao, *Materials Research Express*, 2019, 6, 045048.
4. Z. Zhou, F. Zhao, C. Wang, X. Li, S. He, D. Tian, D. Zhang and L. Zhang, *Optics Express*, 2022, 30, 29749-29759.
5. B. Tan, G. Luo, Z. Zhang, J. Jiang, X. Guo, W. Li, J. Zhang and W. Wang, *Materials Science in Semiconductor Processing*, 2021, 134, 106008.
6. N. Yamada, Y. Kondo and R. Ino, *physica status solidi (a)*, 2019, 216, 1700782.
7. K. R. Chauhan and D. B. Patel, *Journal of Alloys and Compounds*, 2019, 792, 968-975.